International Journal of Infrared and Millimeter Waves, Vol. 12, No. 4, 1991

ELECTRON PROPERTIES IN GaAs FOR THE DESIGN OF MM-WAVE IMPATTs

Heribert Eisele

Center for High-Frequency Microelectronics
Department of Electrical Engineering & Computer Science
The University of Michigan
2245 EECS Building
Ann Arbor, Michigan 48109-2122

Received February 16, 1991

Abstract

A very staightforward method has been developed to apply space-charge resistance measurements for determining the high-field drift velocity of electrons in GaAs. The breakdown voltages of the single-drift flat-profile IMPATT diodes used in these measurements justify the validity of well known ionization rates for still higher electric fields.

1. Introduction

GaAs IMPATT diodes for frequencies around 94 GHz and higher[1] operate in the active region with a maximum electric field E above 800 $kVcm^{-1}$. At these fields any systematic experimental values for drift velocities v_{dn}, v_{dp} and ionization rates α_n, α_p of electron and holes especially at elevated temperatures have not been reported. So far, two methods have been used to determine the drift velocity of electrons in GaAs, the time-of-flight method[2-5] giving very precise data only up to 234 $kVcm^{-1}$ and the method using the space-charge resistance[6] R_{sc}. Neither the well known equation for the space-charge resistance[7] nor a more sophisticated method[8] take into account that v_{dn} monotonically decreases for high electric fields according to theoretical[9-11] and experimental results[2-6].

Since a short and well defined avalanche region does not exist for single-drift W-band IMPATT diodes as already discussed[12], the avalanche region considerably influences R_{sc}. Therefore a very straightforward method has been developed to calculate R_{sc} from the basic continuity and Poisson's equations using different velocity vs. field profiles.

0195-9271/91/0400-0345$06.50/0

2. Static approximation for the space-charge resistance

In order to include the effect of the avalanche region it is assumed that R_{sc} measured at f above the thermal cut-off frequency can be derived from the static I/V-characteristic excluding thermal effects,

$$R_{sc} = \left.\frac{dV}{dI}\right|_{I=I_B} \tag{1}$$

where I_B is the bias current.

If diffusion effects are neglected in the space-charge region, the equation for the electron current density J_n as a function of space x from $-w_p$ to w_n, bias current I_B and active device area A_D can be written as[6]

$$\frac{J_n(x)A_D}{I_B} = \exp\int_{-w_p}^{w_n}[\alpha_n(x)-\alpha_p(x)]dx \cdot \int_{-w_p}^{w_n}\alpha_p(x)\exp\int_{-w_p}^{x}[\alpha_p(x')-\alpha_n(x')]dx'dx \tag{2}$$

with $\alpha_n(x) = \alpha_n(E(x))$ and $\alpha_p(x) = \alpha_p(E(x))$.

The most recent paper on ionization rates[13] includes a dead space correction[14] for an energy below the threshold W_{th} in the dead space region of length d (q: electron charge).

$$\alpha_n(x) = 0 \text{ for } q\int_{-w_p}^{-w_p+d} E(x)dx \leq W_{th} \tag{3}$$

Eq. (3) was used for the ionization rates where applicable, otherwise W_{th} was set to zero.

The integration of Poisson's equation gives

$$E(x) = \frac{q}{\epsilon_r\epsilon_0}\int_{-w_p}^{w_n}\left[N_D(x) - N_A(x) + \frac{J_c - J_n(x)}{qv_{dp}(x)} - \frac{J_n(x)}{qv_{dn}(x)}\right]dx \quad , \tag{4}$$

whereby $v_{dn}(x) = v_{dn}(E(x))$, $v_{dp}(x) = v_{dp}(E(x))$, $J_cA_D \approx I_B$, $N_D(x) - N_A(x)$ is doping concentration and $\epsilon_r\epsilon_0$ the semiconductor permittivity. Intergrating eq. (4) and taking the built-in voltage[7] V_{bi} into account gives the voltage V at the terminals.

$$V = \int_{-w_p}^{w_n} E(x)dx - V_{bi} \tag{5}$$

Eq. (1) to (5) were solved numerically whereby in eq. (4) three different curves for velocity-field dependence were assumed as shown in Fig. 1. At fields below 234 $\mathrm{kVcm^{-1}}$ all three were based upon the well matching experimental values[2–5] in the literature, the values above were generated from a hyperbolic decrease comparable to simulations[9,10]. For the drift velocity of holes v_{dp} experimental values[15] below 100 $\mathrm{kVcm^{-1}}$ and theoretical values[16] above 100 $\mathrm{kVcm^{-1}}$ were applied. Since holes mainly occur in the avalanche region, changes in the velocity

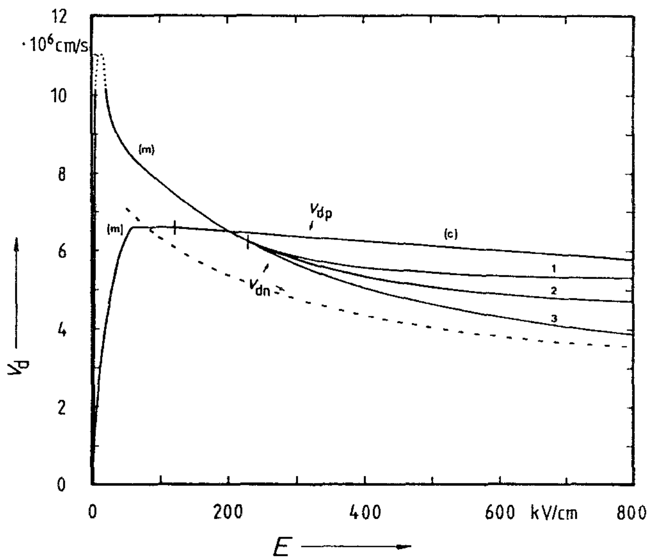

Fig. 1: Drift velocities v_{dn}, v_{dp} of electrons and holes vs. the electric field E
—: $T_0 = 300$ K
(m): measured characteristics[2–5,15] ($T_0 = 300$ K)
(c): calculated curve ($T_0 = 300$ K)
- -: extrapolated curve for $T = 500$ K.

vs. field profile of holes only slightly influence the solution of eq. (1) to (5).

3. Measurement set-up

The expected value range for R_{sc} according to eq. (1) lies between about 0.5 Ω and 10 Ω. Therefore, a fixture having a low series resistance and series inductance was used to determine the low-frequency (LF) impedances $\underline{Z}_f$, $\underline{Z}_r$ of the IMPATT diode in both the forward and reverse (breakdown) directions. The residual series resistance (< 5 mΩ) and inductance ($\ll 10$ nH) were evaluated by replacing the diode with a short and thereafter with a precise resistor and they were factored out for the actual measurement by the computer program.

Fig. 2 shows the schematic circuit diagram of the measurement set-up including the bias circuit for the IMPATT diode (R_1, R_2, C_1, C_2 and C_3). The reference resistor R_3 and the IMPATT diode D form a voltage divider, R_4 and R_5 ensure decoupling and impedance matching. The low-noise broadband amplifier VV in parallel with the terminals of the diode had an input impedance above 1 kΩ and was provided to measure the open-circuit noise voltage at the breakdown.

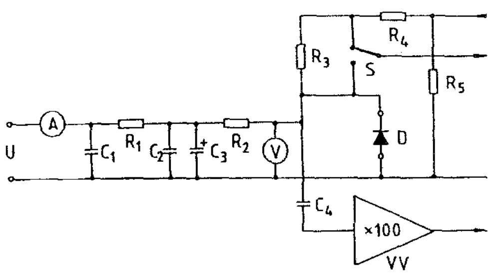

Fig. 2: Schematic diagram of the bias circuit and the impedance evaluation circuit.
D: IMPATT diode
VV: AD 9611
R_1: 50 Ω R_2: 50 Ω R_3: 50 Ω R_4: 510 Ω R_5: 56 Ω
C_1: > 10 μF C_2: 10 μF C_3: > 4700 μF C_4: > 10 μF

4. Experimental results

Several ionization rates reported in the literature[13] were extrapolated to higher electric fields and the calculated breakdown voltages compared to the experimental ones of single-drift flat-profile IMPATT diodes with their abrupt pn-junction. As can be seen in Fig. 3 excellent agreement was found for ionization rates given by Bulman et al.[13]. For this reason these ionization rates and their extrapolations were exclusively used in the following theory-experiment comparision.

Fig. 4 shows the absolute value of the diode impedance $\underline{Z}_r$ as a function of frequency f. For $f < 100$ Hz $|\underline{Z}_r|$ mainly consists of the thermal resistance R_{th1} (due to the heat-flow resistance[17] r_w), the space-charge resistance R_{sc} and the diode series resistance R_s, but for $f > 30$ MHz $|\underline{Z}_r|$ reduces to R_{sc} and the diode series resistance R_s closely enough. R_s was determined in the forward direction for $f > 30$ MHz where the absolute value of diode impedance $\underline{Z}_f$ consists of R_s, the resistance R_{ud} of the undepleted region w_s and the small-signal impedance R_d of the pn-junction. In GaAs the diffusion capacitance can be neglected at these frequencies and the operating bias current I_f, and, therefore,

$$R_d = \frac{kT_j}{qI_f} \quad , \tag{6}$$

$$R_{ud} = \frac{w_s}{\sigma A_D} \quad , \tag{7}$$

whereby σ is the conductivity in the active region of the diode, k the Boltzmann constant and T_j the junction temperature.

It should be noted[18] that essentially for $f < 100$ Hz

$$\underline{Z}_f = R_{th2} + R_s + R_{ud} + R_d \tag{8}$$

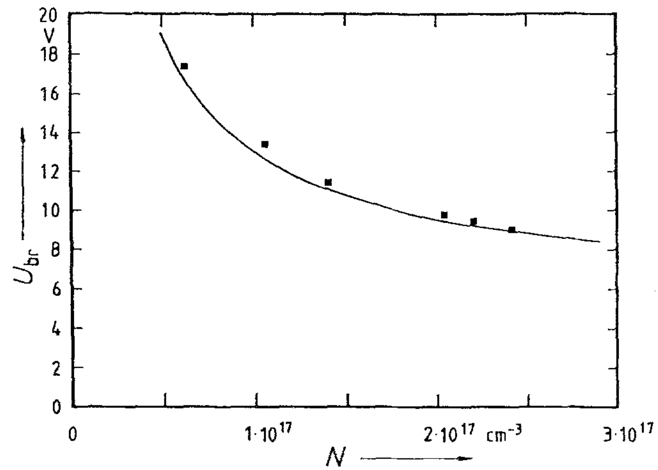

Fig. 3: Breakdown voltage U_{br} of an abrupt pn-junction as a function of the doping concentration N in the n-type layer.

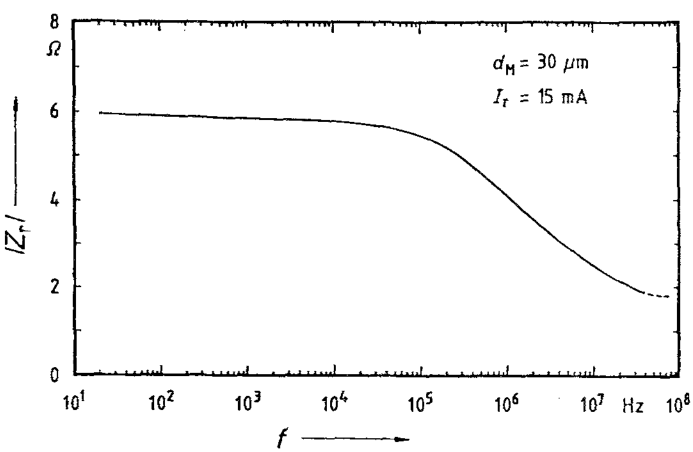

Fig. 4: Absolute value of the small signal diode impedance $\underline{Z}_r$ at breakdown ($I_B = I_r$) as a function of the frequency f (d_M: diode diameter).

has the additional negative thermal resistance R_{th2} due to the heat-flow resistance r_w as can be seen in Fig. 5. R_{th2} can be roughly evaluated[18] (with β_d: temperature coefficient of the forward voltage V_d) to

$$R_{th2} \approx \beta_d r_w (V_d + 2R_d I_f) \quad . \tag{9}$$

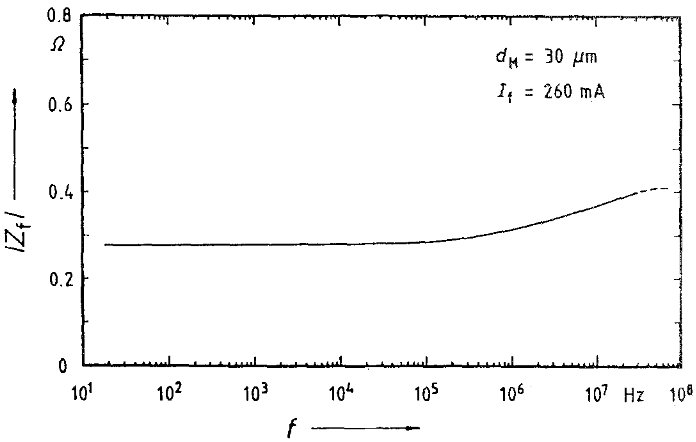

Fig. 5: Absolute value of the small signal diode impedance $\underline{Z}_f$ in forward direction at I_f as a function of the frequency f (d_M: diode diameter).

Low-frequency noise measurements[17] as shown in Fig. 6 were used to characterize the uniformity of the breakdown, and Fig. 7 together with Fig. 6 clearly depicts that uniform breakdown is reached at current densities about 2 kAcm^{-2}, which is comparable to values reported before[8]. For this bias the temperature increase is below 10 K for diodes on diamond heat sinks and below 20 K for diodes on copper heat sinks and, therefore, it can be neglected. For higher current densities $|\underline{Z}_r|$ increases because the junction temperatures raises, the space-charge region widens[12], and the current is more displaced off the center to the border of the device area.

Finally Fig. 8 presents R_{sc} as a function of the doping concentration $N_D - N_A$ in the active region for the three velocity vs. field profiles shown in Fig. 1. The measured space-charge resistances of single-drift flat-profile IMPATT diodes with six different doping levels in the active region ranging from 6.3×10^{16} cm^{-3} to 2.4×10^{17} cm^{-3} (Q-band to V-band[20,21], W-band[1]) are in excellent agreement with the calculated curve 2 that goes from 6.3×10^6 cms^{-1} at 215 kVcm^{-1} down to 3.8×10^6 cms^{-1} at 800 kVcm^{-1} for a temperature of 300 K. Furthermore, this curve also agrees very well with the recent results of a detailed Monte-Carlo simulation[11]. The doping concentration in the active region was determined by

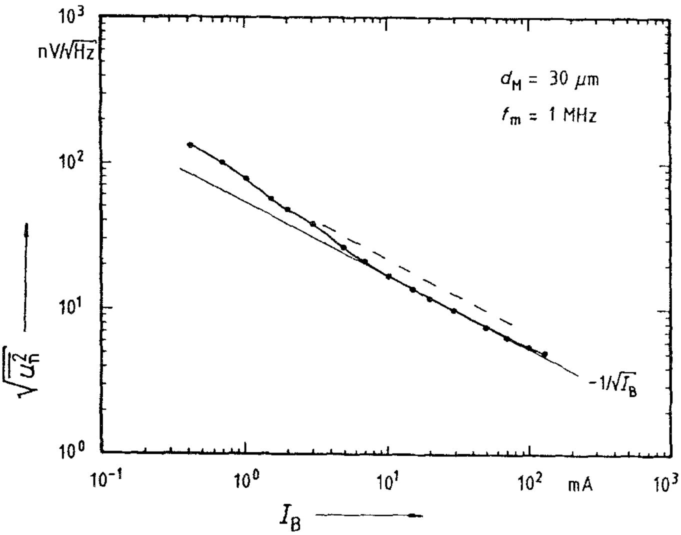

Fig. 6: Open circuit noise voltage per unit bandwidth vs. bias currrent I_B at breakdown (measuring frequency $f \approx 1$ MHz).

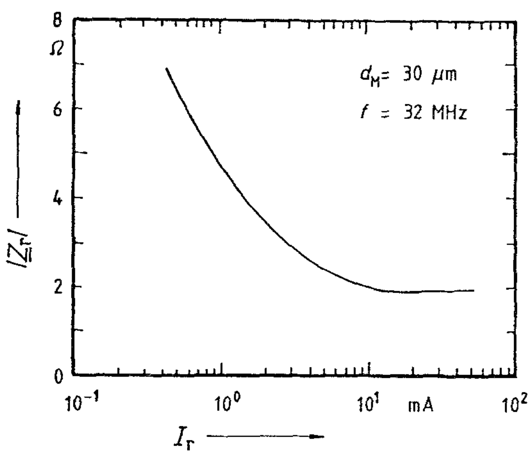

Fig. 7: Absolute value of the small signal diode impedance $\underline{Z}_r$ at breakdown as a function of the bias current I_B.

standard CV-profiling and precise electrochemical profiling[19] using the Polaron PN 4200.

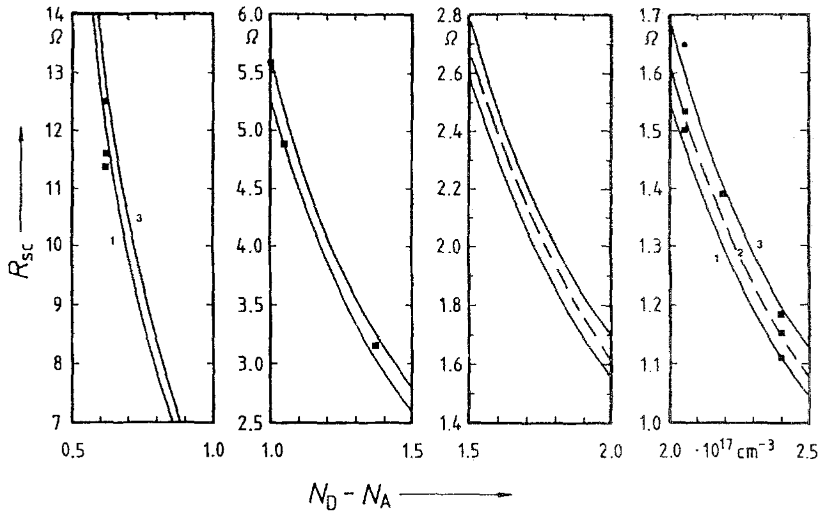

Fig. 8: Space charge resistance R_{sc} vs. doping concentration $(N_D - N_A)$ of the active n-doped layer at $T = 300$ K, for $A_D = 1 \times 10^{-5}$ cm^{-2}, $I_B = 20$ mA and the three $v_{dn}(E)$-profiles 1, 2, 3 of Fig. 1.
■ : measured values, plotted as $R_{sc}\pi d_M{}^2/4 \times 10^{-5}$ cm^{-2} (d_M: diode diameter).

From the curve 2 for $T_0 = 300$ K in Fig. 8 the drift velocity at $T = 500$ K has been extrapolated and used together with the extrapolated ionization rates for the design of W-band single-drift flat-profile IMPATT diodes. As state-of-the-art in GaAs these diodes delivered an output power up to 320 mW at an efficiency of 6.0 % for an oscillation frequency about 95 GHz[22].

5. Conclusion

The excellent agreement of measured and calculated breakdown voltages for the abrupt pn-junction of GaAs single-drift flat-profile IMPATT diodes justify the extrapolation of well known ionization rates to electric fields up to about 850 kVcm^{-1}. A straightforward method to calculate space-charge resistances implies field dependent drift velocities of electrons and holes. For the first time, this method is capable to give a clue for the velocity vs. field profile of electrons up to 800 kVcm^{-1}. The good agreement between these experimental results and theoretical curves confirm those results obtained from Monte-Carlo simulations. Both results, ionization rates and drift velocities, are a useful starting-point in designing IMPATT diodes for frequencies above 100 GHz.

6. Acknowledgments

Most of the measurements and calculations were performed at the Lehrstuhl für Allgemeine Elektrotechnik und Angewandte Elektronik, Technical University Munich. The work was partially supported by the Frauenhofer Gesellschaft. Special thanks go to Xiangkun Zhang for making the IMPATT diodes and results of his thesis available to me. The author thanks Helmut Grothe for supplying the high-quality MBE material. Discussions with Prof. Harth are gratefully appreciated.

7. References

1. Eisele, H.: "Selective etching technology for 94 GHz GaAs IMPATT diodes on diamond heat sinks", *Solid-State Electronics*, **32**, 1989, pp. 253–257.

2. Ruch, J. G., Kino, G. S., "Transport Properties of GaAs", *Phys. Rev.*, **174**, 1968, pp. 921–931.

3. Houston, P. A., Evans, A. G. R., "Electron drift velocity in n-GaAs at high electric fields", *Solid-State Electron.*, **20**, 1977, pp. 197–204.

4. Smith, P. A., Inoue, M., Frey, J., "Electron velocity in Si and GaAs at very high electric fields", *Appl. Phys. Lett.*, **37**, 1980, pp. 797–798.

5. Windhorn, T. H., Roth, T. J., Zinkiewicz, L. M., Gaddy, O. L., Stillman, G. E., "High field temperature dependent drift velocities in GaAs", *ibid.*, **40**, 1982, pp. 513–515.

6. Okamoto, H., Ikeda, M., "Measurement of the Electron Drift Velocity in Avalanching GaAs Diodes", *IEEE Trans. Electron Devices*, **ED-23**, 1976, pp. 372–374.

7. Sze, S. M., *Physics of Semiconductor Devices*, 2nd Ed., J. Wiley & Sons, New York, 1981, pp. 1–868.

8. Glover, G. H., Tantraporn, W., "Doping profile measurements from avalanche space-charge resistance: a new technique", *J. Appl. Physics*, **46**, 1975, pp. 867–874.

9. Shichijo, H., Hess, K., "Band-structure-dependent transport and impact ionization in GaAs", *Phys. Rev. B*, **23**, 1981, pp. 4197–4207.

10. Lippens, D., private communication.

11. Fischetti M. V., Laux S. E., "Monte Carlo analysis of electron transport in small semiconductor devices including band-structure and space-charge effects", *Phys. Rev. B*, **38**, 1988, pp. 9721–9745.

12. Eisele H., "GaAs W-band IMPATT diodes - the first step to higher frequencies", to be published in *Microwave Journal*, 1990.

13. Bulman, G. E., Robbins, V. M., Stillman, G. E., "The Determination of Impact Ionization Coefficients in (100) Gallium Arsenide Using Avalanche Noise and Photocurrent Multiplication Measurements", *IEEE Trans. Electron Devices*, **ED-32**, 1985, pp. 2454–2466.

14. Okuto, Y., Crowell, C. R., "Threshold energy effects on avalanche breakdown voltage in semiconductor junctions," *Solid-State Electron.*, **18**, 1975, pp. 161–168.

15. Holway, L. H., Steele S. R., Adlerstein, M. G., "Measurement of electron and hole properties in p-type GaAs", Proc. of the Seventh Biennial Cornell Electrical Engineering Conference, 1979, pp. 199–208.

16. Brennan, K., Hess, K., "Theory of high field transport of holes in GaAs and InP", *Phys. Rev. B*, **29**, 1984, pp. 5581–5590.

17. Haitz, R. H., Stover, H. L., Tolar, N. J., "A method for heat low resistance measurements in avalanche diodes", *IEEE Trans. on Electron. Devices*, **ED-16**, 1969, pp. 438–444.

18. Eisele, H., "Theorie, Technologie und Untersuchung von Lawinenlaufzeitdioden aus MBE-GaAs für W-Band Frequenzen", Ph.D. Thesis, Technical University of Munich, 1989.

19. Eisele, H., "Reproducible and accurate electrochemical doping profile measurements in GaAs", to be published in *Archiv der elektr. Übertragung*, 1990.

20. Zhang, X., "Herstellung und Untersuchung von GaAs Lawinenlaufzeitdioden für 60 GHz", Ph.D. Thesis, Technical University of Munich, 1984.

21. Zhang, X., private communication.

22. Eisele H., Grothe H., "GaAs W-band IMPATT diodes made from MBE material", Proceedings of the MIOP '89, Sindelfingen, Feb. 28 - March 2 1989, Session 3A.6.